Chapter 6

Magneto-ionic control of spin polarization in multiferroic tunnel junctions

Y. Wei, S. Matzen, C. P. Quinteros, T. Maroutian, G. Agnus, P. Lecoeur & B. Noheda,
npj Quantum Materials (2019) (Accepted)

Abstract

Multiferroic tunnel junctions (MFTJs) with $Hf_{0.5}Zr_{0.5}O_2$ barriers are reported to show both tunneling magnetoresistance effect (TMR) and tunneling electroresistance effect (TER), displaying four resistance states by magnetic and electric field switching (see Chapter 5). Here we show that, under electric field cycling of large enough magnitude, the TER can reach values as large as 10^6%. Moreover, concomitant with this TER enhancement, the devices develop electrical control of spin polarization, with sign reversal of the TMR effect. Currently, this intermediate state exists for a limited number of cycles and understanding the origin of these phenomena is key to improve its stability. The experiments presented here point to the magneto-ionic effect as the origin of the large TER and strong magneto-electric coupling, showing that ferroelectric polarization switching of the tunnel barrier is not the main contribution.

6.1 Introduction

Combining the TMR effect of magnetic tunnel junctions (MTJs) with additional functionalities provided by the tunnel barrier, i.e. using multiferroic[1] or ferroelectric[2, 3] layers as barriers, has drawn considerable attention driven by their potential application in multilevel memories. In these devices, four resistance states are achieved by means of both the TMR (resistance change induced by magnetic field switching) and the TER (resistance change by electric switching) effects.[4–6] In addition, by combining two ferroic orders (ferromagnetic and ferroelectric), the coupling between the magnetic and electric degrees of freedom could realize electric field controlled spintronics, promising for the development of low-power and fast devices.[6–13]

The magnetoelectric (ME) coupling in heterostructures can have different origins. For instance, in artificial multiferroics made of ferroelectric and ferromagnetic layers, the ME coupling can be either strain-mediated or charge-mediated.[14] The displacement of atoms under applied electric field in the ferroelectric barrier can affect the interface magnetization due to

hybridization. In addition, the magnetization of the ferromagnet, which is elastically coupled to the ferroelectric, can also change upon application of electric field due to magnetoelastic coupling.[15–17] Alternatively, accumulation of spin-polarized carriers at the interface upon polarization of the dielectric [18–20] can also give rise to ME coupling. This effect is enhanced in the case of a ferroelectric, as a larger number of carriers will typically be necessary for screening.[21–24]. More recently, the magneto-ionic effect[25] has been proposed, by which the applied electric field induces ion migration, modifying the interfaces of the heterostructures and the properties of the layers.

In this work, tunnel barriers of crystalline $Hf_{0.5}Zr_{0.5}O_2$ (HZO) are used in MTJs. Crystalline HZO grown under certain conditions has shown nanoscale ferroelectricity.[26, 27]. Epitaxial growth of crystalline HZO can also be achieved[28] and has been recently also demonstrated on perovskite substrates with $La_{0.7}Sr_{0.3}MnO_3$ (LSMO) as bottom elecrode[29–31]. The large band gap and high resistance of the HZO layer allows to fabricate full devices with extended electrodes for wire bonding, despite the low thickness of the barrier. This is not possible with perovskite ferroelectric (FE) tunnel barriers with such small thickness and, thus, so far these devices have been limited to investigation by scanning probes.[32] Four resistance states have been obtained in this type of junctions by both magnetic and electric field switching, but no ME coupling was reported.[32] Here we show that electric field cycling of high enough amplitude induces irreversible changes in the junction, which evolves from a negligible ME coupling state into a large ME coupling state. In the latter, sign reversal of the TMR effect is achieved by electrical switching reversibly. Concomitantly, with increasing number of cycles, the TER increases to values up to 10^6%. In the following we discuss the mechanisms that lead to such phenomena.

6.2 Experimental methods

Thin films of $Hf_{0.5}Zr_{0.5}O_2$ (HZO) barrier with thickness of 2 nm were grown by pulsed laser deposition (PLD) on FM $La_{0.7}Sr_{0.3}MnO_3$(LSMO)-buffered (001)-$SrTiO_3$ substrates. The thickness of LSMO film is around 30 nm. Details of the growth conditions can be found in *Chapter 3*. 50 nm FM Cobalt with a protective layer of Au (50nm), to preserve Co from oxidation, were deposited by sputtering on top of the HZO layer, to form the junctions with LSMO (FM) / HZO (FE)/ Co (FM) stacks. Junctions with different sizes, ranging from $10\mu m \times 10\mu m$ to $30\mu m \times 30\mu m$, are fabricated (see details in *Chapter 5*). The electrical measurements are performed using a Keithley 237 source measurement unit and a Keithley 4200A-SCS parameter analyzer, and the temperature environment and magnetic field are supplied by a Physical Properties Measurement System (PPMS) by Quantum Design. As shown in the schematic drawing in Fig. 6.1(a), the voltage source is applied on the LSMO/HZO/Co stack with bottom electrode grounded (for a positive bias, the electrons are tunneling from LSMO to Co). The magnetic field is swept along the easy magnetization axis of LSMO in the [110] direction. As reported in *Chapter 5*, the large band gap and high resistance of the HZO layer allows to fabricate full devices with extended electrodes for wire bonding, despite the low thickness of the barrier. This is not possible with perovskite ferroelectric (FE) tunnel barriers with such

small thickness and, thus, so far these devices have been limited to investigation by scanning probes.

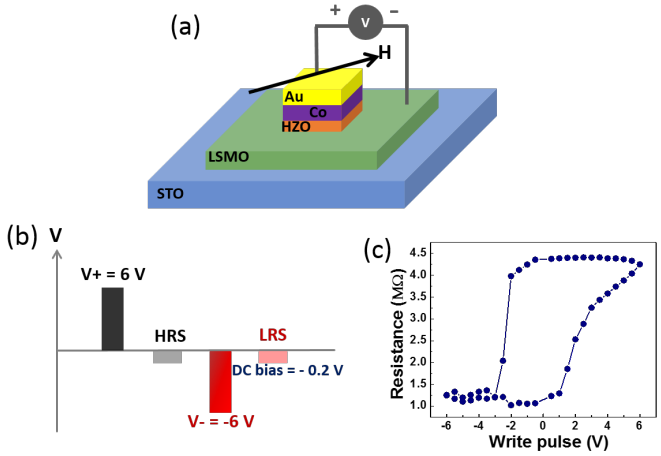

Figure 6.1: *(a) Schematic drawing of a tunnel junction device, with bottom electrode grounded. The heterostructure is grown on a 001-oriented $SrTiO_3$ substrate. The applied magnetic field is along the [110] direction; (b) electrical pulses of 6 V with both positive (black) and negative (red) polarity and 500 μs duration are applied to the junctions in order to bring them into the high (HRS) and low resistance state (LRS), respectively. All TMR loops are measured under a DC bias of -0.2 V, both in the HRS and LRS; (c) changes in resistance under the application of different amplitude of electrical pulses in the same junction, as shown in Fig. 5.6(a) in Chapter 5.*

6.3 Results and discussion

6.3.1 Electrical switching of spin polarization

By the electrical pulse switching protocol shown in Fig. 6.1(b), the junction switches between the high resistance state, HRS (R_H, after V+ pulse) and the low resistance state, LRS (R_L, after V- pulse). A voltage pulse with amplitude as large as 6 V is used in order to obtain the maximum resistance contrast (TER $\sim 400\%$) (see Fig. 6.1(c) and ref.[32]). This resistance change is consistent with the change in the barrier height that is expected upon the switching of the ferroelectric polarization of the tunnel barrier,[1] giving rise to a HRS for polarization pointing towards the LSMO layer, and to the LRS for polarization pointing towards the Co layer. It is interesting to notice that LSMO/HZO/Pt junctions, fabricated by M. C. Sulzbach et al.[33] with the same material as tunnel barrier but with a double barrier thickness, also

show TER values of around 400%. This TER is reproducible with cycling under relatively smaller driving voltages ($\sim$ 1 MV/cm), also suggesting that this contribution arises from the ferroelectric polarization.

In both HRS and LRS, TMR loops are obtained, as shown in Fig. 6.2, leading to four resistance states ($R_{H\uparrow\uparrow}$, $R_{H\uparrow\downarrow}$, $R_{L\uparrow\uparrow}$, $R_{L\uparrow\downarrow}$, where the arrows signal the relative orientation of the electrodes magnetization). During the first few cycles, the TMR effect of the HRS ($\sim$ 6.2%) and LRS ($\sim$ 5.4%) are similar in magnitude (see Fig. 6.2(a)), indicating a negligible ME coupling, which differs from the strong coupling reported in perovskite tunnel barriers [12, 34, 35]. This stage, which we name stage A, is the one reported in ref.[32]. Interestingly, after a few tens of cycles, the behaviour changes substantially, reaching the stage B, as shown in Fig. 6.2(b): the TMR sign is reversed from positive (HRS) to negative (LRS) indicating that the spin polarization is switched by the external electric field in a reversible manner, as shown in Fig. 6.3. In addition, the coercive field of the harder ferromagnet (the Co layer) in the LRS (with negative TMR) increases by, approximately, a factor of two, compared to the switching fields of the HRS (with positive TMR). Moreover, the switching becomes sharper in the LRS. The increase of the coercive field and steep switching of the Co layer upon electrical cycling could originate in a modification of the HZO/Co interface.[25]. The number of cycles needed to reach the stage B has been found to differ depending on the junction under investigation. (For the specific device studied in the work, the junction at stage A/B/C are measured after $\sim$20/75/110 cycles, respectively.)

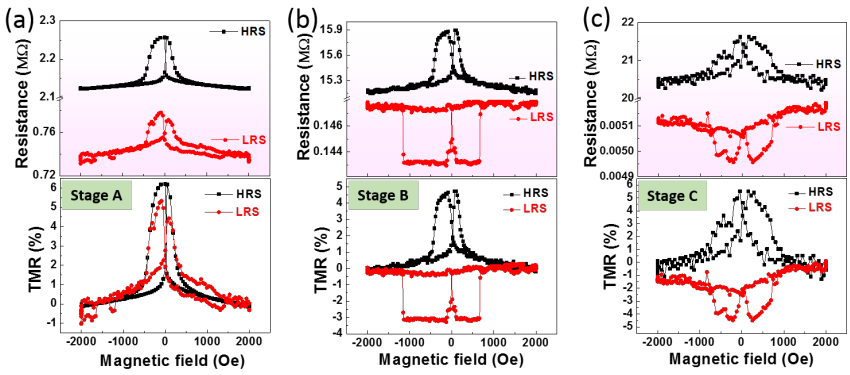

Figure 6.2: *(a)-(c) Resistance as a function of sweeping magnetic field (top panels) and TMR ratio (bottom panels) in the HRS (black squares) and LRS (red circles) measured at three different intermediate stages (named as stage A, B and C, respectively) upon repeated application of +/-6V electric pulses. Measurements shown here are performed at 50 K on a junction device with an electrode area of* $30\mu m \times 30\mu m$.

With further electric cycling (stage C), the TMR signal becomes more noisy, as observed in Fig. 6.2(c). The switching magnetic fields for the direct and reversed TMR become comparable but still higher than those of stage A (Fig. 6.2(a)). However, the magnitude of the TMR effect

is not substantially altered. In the meantime, the two magnetic states are less well defined with less abrupt magnetic switching than the previous two stages, which could indicate an increasing number of defects introduced in the stack. For longer cycling time, with number of cycles depending on the junction, the TMR effect eventually disappears but the TER effect is still present.

The TMR sign has been reported to reverse by modification of the Co interface, either by adding an interface layer[36, 37], or by the electric field-controlled hybridization at the interface (modified by the different ferroelectric polarization states)[34]. These mechanisms affecting the Co/barrier interface are consistent with the changes, described above, of the magnetization switching of the Co layer upon electric cycling. However, since the reversed TMR is not observed in the A-stage (it only appears upon repeated electric cycling), the ferroelectric polarization switching can be discarded as the main contribution to the TMR sign reversal. Moreover, changes in the junctions by the introduction of oxygen vacancies (V_O^{2+}) have also been reported to promote TMR sign reversal[38]. Given the possibility for positively charged V_O^{2+} to migrate back and forth under the application of the electric field pulses with opposite polarities, we propose that ionic exchange is responsible for the observed changes of spin polarization, as well as the modification of the Co-HZO interface upon cycling.[25, 39, 40].

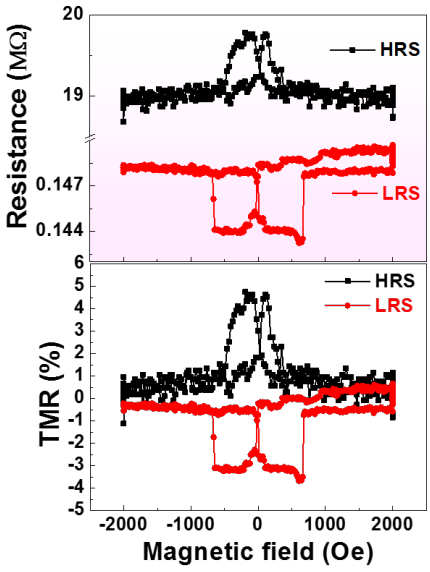

Figure 6.3: *Second run of electrical switching of spin polarization at stage B.*

6.3.2 Loss of bias-induced TMR sign change

Focusing on stage C, from the I-V curves measured in parallel and anti-parallel magnetic states, we plot the bias dependence of the TMR for both HRS and LRS in Fig. 6.4. A striking feature is that in HRS state the TMR exhibits a very weak bias-dependence and it is always positive; while in the LRS, the TMR is always negative with a rapid drop of TMR with increasing bias (absolute value), characteristic of thin-film MFTJs and attributed to spin-flip scattering [41]. The electric field switching of spin polarization is, thus, evidenced over the whole investigated voltage range. Tuning of the read voltage allows to select the magnitude of the TMR change (e.g. Fig. 6.2(c) for -0.2 V read voltage). Looking at the bias-dependence of the TMR in the as-grown state for the same device (Fig. 6.4, inset), and noting that similar curves are obtained in both HRS and LRS at stage A for different junctions [32], it is clear that electric field cycling completely changes the control of the spin polarization of the tunneling electrons. While the initial stage A shows a read voltage-controlled TMR sign change, already reported for Co-based junctions[32, 42, 43], in stage C the TMR sign is wholly determined by the switchable resistance state of the device.

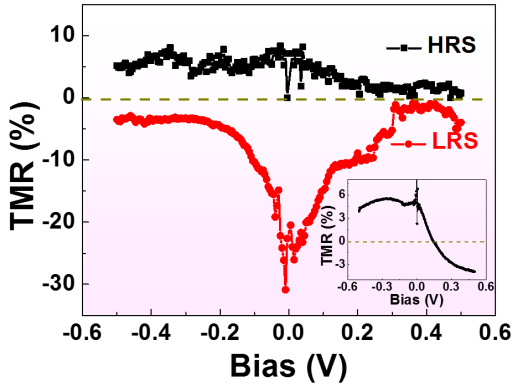

Figure 6.4: *Bias dependence of TMR measured at stage C for the HRS and LRS, showing electrical switching of spin polarization, on the device shown in Fig. 6.2(c), with size of* $30\mu m \times 30\mu m$*, measured at 50 K. The inset shows the bias dependence of TMR in the as-grown state (before any electrical cycling) on the same device. Similar curves are obtained in both HRS and LRS at stage A for a* $20\mu m \times 20\mu m$ *junction, as shown in ref. [32].*

6.3.3 TER built-up

Concomitantly, the resistance ratio between the HRS and LRS (TER) also increases substantially upon electric field cycling. By measuring the current-voltage (I-V) curves after positive and negative electric pulses, we can extract the TER at different bias by measuring the cur-

rent ratio of HRS and LRS (I_L/I_H). TER rises from $10^2\%$ to $10^6\%$ (stage A to C) with a large number of intermediate states, as shown in Figs. 6.5(a)-(c), corresponding to Figs. 6.2(a)-(c), respectively.

Thus, it is shown that the junctions are strongly affected by the very large electric fields applied across the ultrathin HZO barrier, which induce stage B and C with highly enhanced magnetoelectric coupling and very large TER, of great interest for devices. The driving voltages required to achieve these stages are close to the junction breakdown field. Therefore, the ability to keep cycling the device with such a large stimulus could be due to a voltage drop somewhere in the device, such as at the Co-HZO interface. Understanding the mechanisms leading to this evolution would crucially help finding the optimal conditions required for applications.

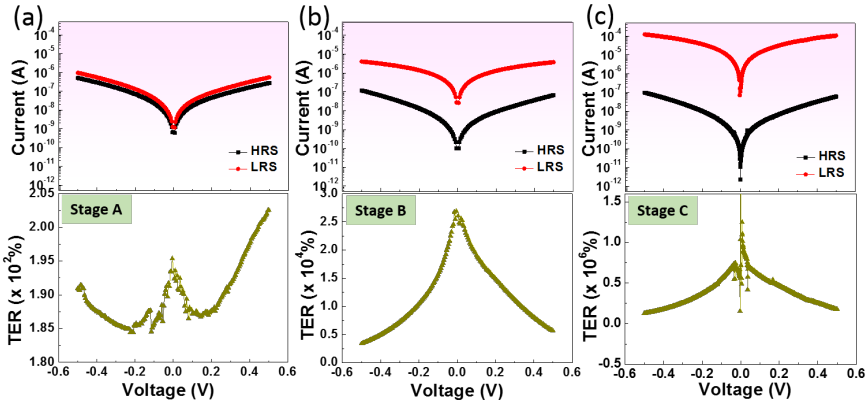

Figure 6.5: *(a)-(c) Current as a function of bias (up panel) in the HRS (black squares) and LRS (red circles) and TER values (down panel) at three different stages A, B, and C, which correspond to Fig. 6.2(a)-(c). All are measured on a $30\mu m \times 30\mu m$ junction at 50 K.*

6.3.4 Ion exchange mechanism

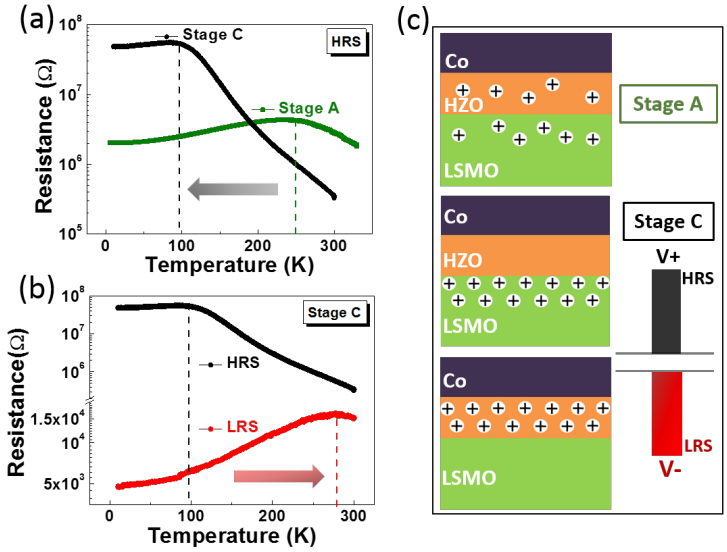

Figure 6.6: *(a) R-T curves in the HRS at stage A (green) and stage C (black), respectively; (b) R-T curves in the HRS (black) and LRS (red) at the stage C; (c) sketch of the proposed model of interface ionic exchange.*

To shed light into the factors affecting the evolution from stage A to C by electric cycling, transport measurements of resistance *versus* temperature (R-T) are shown in Fig. 6.6(a). The same junction is measured in the HRS in stage A (green) and stage C (black). In stage A, a metal-insulator transition happens at around 250 K. This is the temperature at which the ferromagnetic/metal-to-paramagnetic/insulator transition of LSMO at the interface with HZO takes place and, thus, where the TMR disappears.[32] Upon electric field cycling, the transition temperature decreases. In Fig. 6.6(a), the resistance of stage C (black) is shown to display the transition at around 100 K, which again coincides with the temperature at which TMR disappears (see Fig. 6.7). The decrease of transition temperature from stage A to C is consistent with an oxygen deficiency at the LSMO interface[38, 44, 45] that increases with repeated electric field cycling. In addition, the junction R_H increases from stage A to C (see Fig. 6.2 and 6.5), which also agrees with an increasing content of oxygen vacancies in the LSMO layer at the HRS upon cycling, since oxygen vacancies are well known to reduce the carrier (hole) concentration in LSMO.[44–47]

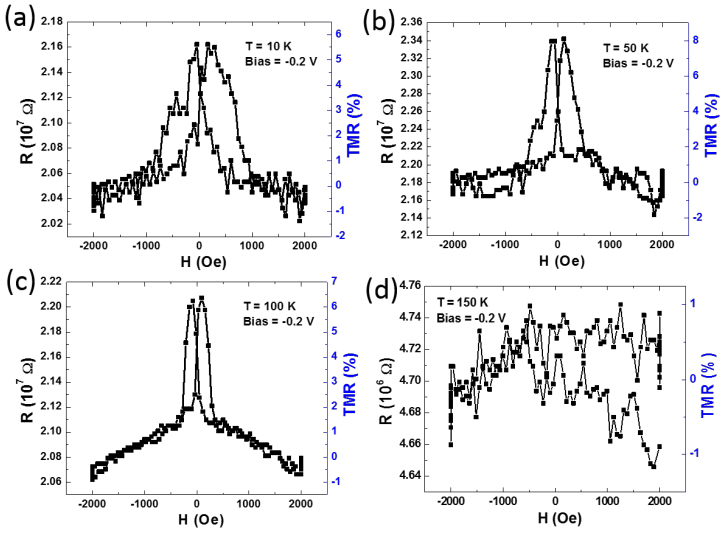

Figure 6.7: *Temperature dependent TMR loops of HRS at stage C. (a) 10 K; (b) 50 K; (c) 100 K; (d) 150 K.*

Furthermore, the R-T measurements at stage C (with large TER and strong ME coupling) in the HRS and LRS are shown in Fig. 6.6(b). The transition temperature at the HRS (black), which had been lowered by the action of electric cycling to $\sim$ 100 K, increases up to $\sim$ 275 K, after the junction is brought to the LRS (red), which is higher than the transition temperature of the stage A ($\sim$ 250 K, see Fig. 6.6(a)). This indicates that by applying a large negative pulse to the junction, the LSMO layer can reach an oxygen content larger than that of the initial stage. This is consistent with ionic exchange of oxygen vacancies in between the LSMO electrode and the HZO barrier during cycling, as represented in Fig. 6.6(c). Giant resistive switching by oxygen vacancies migration has also been observed in different ferroelectric oxides tunnel barriers[48].

- **Large TER**

In Fig. 6.6(c), we illustrate this possible scenario: in the as-grown state, both the LSMO and the HZO layers contain V_O^{2+} (top panel). Upon electric field cycling, V_O^{2+} are driven back and forth across the barrier. The evolution of the TER from 10^2% to 10^6% can be explained by the accumulation of the oxygen vacancies at the vicinity of the HZO/LSMO interface, thus increasing the V_O^{2+} concentration that participates in the ionic exchange process. In this picture, the HRS is due to the oxygen vacancies being pushed into the LSMO electrode, resulting in a very resistive HZO/$La_{0.7}Sr_{0.3}MnO_{3-\delta}$ contact. The LRS is obtained with the oxygen vacancies drifting back into the HZO barrier upon negative voltage pulse application, greatly

reducing the resistivity of the junction[49]. This gives rise to highly different current levels between HRS and LRS (large TER) as shown in Fig. 6.5(c) and Fig. 6.8(a). Still, for both states, the non-linear I-V curves are similar (Fig. 6.8(a)) and the shape of the differential conductance curves (Fig. 6.8(b)) is compatible with tunneling conduction[50], ruling out a drastic change of the conduction mechanism as probed by the investigated range of applied voltage.

An open question is the role of the ferroelectric polarization switching in these devices. Resistive switching by electric field has been reported in a wide variety of oxides[49, 51, 52], including binary oxides.[53–55] In the case of ferroelectric tunnel barriers, the profile of the electronic barrier can be modified by polarization reversal, thus causing strong TER effect. [2, 56] In this picture, the increase of TER effect upon cycling could indicate a concomitant increase of the ferroelectric polarization. This effect has been often observed in hafnia-based ferroelectrics (wake-up effect).[57, 58] Even though our thicker films (down to 5 nm-thick) have not shown that effect,[29] we are not able to discard its existence in the present 2 nm tunnel barriers. However, as mentioned earlier, the HRS in the stage A corresponds to downward polarization in Fig. 6.1(c).[32] Upon evolving into stage C, this downward polarization should induce the migration of the oxygen vacancies towards the Co electrode in order to help to screen the polarization charges. However, we observe the contrary: accumulation of oxygen vacancies at the LSMO electrode in the HRS (Fig. 6.6(c)) and, thus, an increase of the ferroelectric polarization upon cycling cannot be the main contribution to the TER build-up. Indeed, due to positively charged oxygen vacancies, the screening ability of the LSMO is expected to decrease, which would increase the depolarizing field and strongly reduce the polarization of the tunnel barrier.

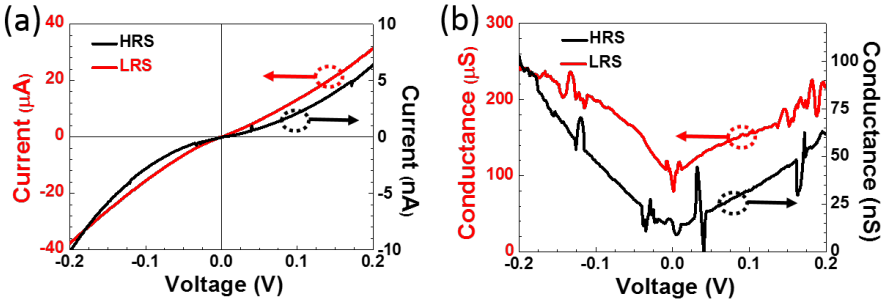

Figure 6.8: *(a) and (b) I-V and dI/dV-V curves, respectively, in the HRS and LRS of stage C measured at 50 K. The spikes observed in the dI/dV curves are a consequence of the small experimental deviations in the experimental I-V data. Notice the different current/conductance scales in the LRS (left axis) and HRS (right axis).*

- **ME coupling**

As discussed above, accompanied by the large TER, a strong ME coupling appears with TMR sign reversal. The reversed TMR has been reported to be due to modification of the Co/tunnel

barrier interface, such as by adding an interfacial layer[36, 37], or by electric field control,[34] similar to our present work. Several microscopic mechanisms have been proposed to explain this phenomenon: a) by hybridization, the magnetic moment of the interfacial ions can be changed strongly by electrical switching[59]; b) the electrostatic contribution at the interface can induce a change of spin polarization in the ferromagnetic layer[60, 61]; and c) electrochemistry (redox of Co) at the interface could also cause a change of magnetization[62]. On the other hand, as shown in Fig. 6.6(b) and 6.6(c), at the HRS (stage C), the LSMO/HZO interface is modified, but the TMR remains the same as at the HRS in stage A (Fig. 6.2(a) and 6.2(c)). Oxygen vacancies at the LSMO/HZO interface, such as described in Fig. 6.6(c), change neither the amplitude nor the sign of the TMR in the HRS, going from stage A to stage C. We, thus, believe that oxygen migration around this LSMO/HZO interface does not play the main role on the TMR sign reversal. Besides changes at the interfaces, a change of localized (defects) states in the barrier can also induce the inversion of TMR sign due to resonant tunneling.[43, 63] For example, in LSMO/STO/Co junctions,[38] changes in the barrier by the introduction of V_O^{2+} have been reported to promote TMR sign reversal. In the stage C of our junction, such a migration of V_O^{2+} in the HZO barrier occurs, back and forth under the application of the high electric field pulses with opposite polarities. Therefore, both the modification of the Co/barrier interface[25] and the resonant tunneling, could contribute to reversal of the TMR sign.

6.4 Conclusion and outlook

In conclusion, TER values of up to $10^6\%$ coexisting with large ME coupling, by which the sign of the TMR effect is reversed with the electric field switching, have been achieved after cycling of LSMO/HZO/Co tunnel junctions with large enough electric fields. These phenomena can be ascribed to the magneto-ionic effect. The temperature dependence of the transport behaviour is consistent with the exchange of oxygen vacancies at the LSMO/HZO interface, together with possible modifications of the HZO/Co interface and change of impurity states of tunnel barrier. Next, an electrical protocol needs to be designed in order to increase the endurance of this state.

Bibliography

[1] M. Gajek, M. Bibes, S. Fusil, K. Bouzehouane, J. Fontcuberta, A. Barthelemy, and A. Fert, "Tunnel junctions with multiferroic barriers," *Nature Materials* **6**(4), p. 296, 2007.

[2] J. Rodríguez Contreras, H. Kohlstedt, U. Poppe, R. Waser, C. Buchal, and N. Pertsev, "Resistive switching in metal-ferroelectric-metal junctions," *Applied Physics Letters* **83**(22), pp. 4595–4597, 2003.

[3] E. Y. Tsymbal, A. Gruverman, V. Garcia, M. Bibes, and A. Barthélémy, "Ferroelectric and multiferroic tunnel junctions," *MRS Bulletin* **37**(2), pp. 138–143, 2012.

[4] J. Scott, "Data storage: Multiferroic memories," *Nature Materials* **6**(4), p. 256, 2007.

[5] N. Hur, S. Park, P. Sharma, J. Ahn, S. Guha, and S. Cheong, "Electric polarization reversal and memory in a multiferroic material induced by magnetic fields," *Nature* **429**(6990), p. 392, 2004.

[6] M. Bibes and A. Barthélémy, "Multiferroics: Towards a magnetoelectric memory," *Nature Materials* **7**(6), p. 425, 2008.

[7] N. Ortega, A. Kumar, J. Scott, and R. S. Katiyar, "Multifunctional magnetoelectric materials for device applications," *Journal of Physics: Condensed Matter* **27**(50), p. 504002, 2015.

[8] J. Webster, "Wiley encyclopedia of electrical and electronics engineering," *Biomedical Instrumentation & Technology* **36**(5), 2002.

[9] W. Eerenstein, N. Mathur, and J. F. Scott, "Multiferroic and magnetoelectric materials," *Nature* **442**(7104), p. 759, 2006.

[10] R. Ramesh and N. A. Spaldin, "Multiferroics: progress and prospects in thin films," *Nature Materials* **6**(1), p. 21, 2007.

[11] M. Fiebig, "Revival of the magnetoelectric effect," *Journal of Physics D: Applied Physics* **38**(8), p. R123, 2005.

[12] V. Garcia, M. Bibes, L. Bocher, S. Valencia, F. Kronast, A. Crassous, X. Moya, S. Enouz-Vedrenne, A. Gloter, D. Imhoff, C. Deranlot, N. Mathur, S. Fusil, K. Bouzehouane, and A. Barthélémy, "Ferroelectric control of spin polarization," *Science* **327**(5969), pp. 1106–1110, 2010.

[13] Y. Yin and Q. Li, "A review on all-perovskite multiferroic tunnel junctions," *Journal of Materiomics* **3**(4), pp. 245–254, 2017.

[14] C. A. Vaz, J. Hoffman, C. H. Ahn, and R. Ramesh, "Magnetoelectric coupling effects in multiferroic complex oxide composite structures," *Advanced Materials* **22**(26-27), pp. 2900–2918, 2010.

[15] J. H. Lee, L. Fang, E. Vlahos, X. Ke, Y. W. Jung, L. F. Kourkoutis, J.-W. Kim, P. J. Ryan, T. Heeg, M. Roeckerath, *et al.*, "A strong ferroelectric ferromagnet created by means of spin–lattice coupling," *Nature* **466**(7309), p. 954, 2010.

[16] K. Wang, J.-M. Liu, and Z. Ren, "Multiferroicity: the coupling between magnetic and polarization orders," *Advances in Physics* **58**(4), pp. 321–448, 2009.

[17] W. Eerenstein, M. Wiora, J. Prieto, J. Scott, and N. Mathur, "Giant sharp and persistent converse magnetoelectric effects in multiferroic epitaxial heterostructures," *Nature Materials* **6**(5), p. 348, 2007.

[18] J. M. Rondinelli, M. Stengel, and N. A. Spaldin, "Carrier-mediated magnetoelectricity in complex oxide heterostructures," *Nature Nanotechnology* **3**(1), p. 46, 2008.

[19] H. Lu, T. A. George, Y. Wang, I. Ketsman, J. D. Burton, C.-W. Bark, S. Ryu, D. Kim, J. Wang, C. Binek, *et al.*, "Electric modulation of magnetization at the batio3/la0.67sr0.33mno3 interfaces," *Applied Physics Letters* **100**(23), p. 232904, 2012.

[20] C. Vaz, Y. Segal, J. Hoffman, R. Grober, F. Walker, and C. Ahn, "Temperature dependence of the magnetoelectric effect in pb(zr0.2ti0.8)o3/la0.8sr0.2mno3 multiferroic heterostructures," *Applied Physics Letters* **97**(4), p. 042506, 2010.

[21] M. Dawber, K. Rabe, and J. Scott, "Physics of thin-film ferroelectric oxides," *Reviews of Modern Physics* **77**(4), p. 1083, 2005.

[22] S. Mathews, R. Ramesh, T. Venkatesan, and J. Benedetto, "Ferroelectric field effect transistor based on epitaxial perovskite heterostructures," *Science* **276**(5310), pp. 238–240, 1997.

[23] S. Wu, S. A. Cybart, D. Yi, J. M. Parker, R. Ramesh, and R. Dynes, "Full electric control of exchange bias," *Physical Review Letters* **110**(6), p. 067202, 2013.

[24] V. Skumryev, V. Laukhin, I. Fina, X. Martí, F. Sánchez, M. Gospodinov, and J. Fontcuberta, "Magnetization reversal by electric-field decoupling of magnetic and ferroelectric domain walls in multiferroic-based heterostructures," *Physical Review Letters* **106**(5), p. 057206, 2011.

[25] U. Bauer, L. Yao, A. J. Tan, P. Agrawal, S. Emori, H. L. Tuller, S. Van Dijken, and G. S. Beach, "Magneto-ionic control of interfacial magnetism," *Nature Materials* **14**(2), p. 174, 2015.

[26] T. Böscke, J. Müller, D. Bräuhaus, U. Schröder, and U. Böttger, "Ferroelectricity in hafnium oxide thin films," *Applied Physics Letters* **99**(10), p. 102903, 2011.

[27] M. H. Park, Y. H. Lee, H. J. Kim, Y. J. Kim, T. Moon, K. D. Kim, J. Mueller, A. Kersch, U. Schroeder, T. Mikolajick, *et al.*, "Ferroelectricity and antiferroelectricity of doped thin hfo2-based films," *Advanced Materials* **27**(11), pp. 1811–1831, 2015.

[28] T. Shimizu, K. Katayama, T. Kiguchi, A. Akama, T. J. Konno, O. Sakata, and H. Funakubo, "The demonstration of significant ferroelectricity in epitaxial y-doped hfo 2 film," *Scientific Reports* **6**, p. 32931, 2016.

[29] Y. Wei, P. Nukala, M. Salverda, S. Matzen, H. J. Zhao, J. Momand, A. S. Everhardt, G. Agnus, G. R. Blake, P. Lecoeur, *et al.*, "A rhombohedral ferroelectric phase in epitaxially strained hf0.5zr0.5o2 thin films," *Nature Materials* **17**(12), p. 1095, 2018.

[30] J. Lyu, I. Fina, R. Solanas, J. Fontcuberta, and F. Sánchez, "Robust ferroelectricity in epitaxial hf1/2zr1/2o2 thin films," *Applied Physics Letters* **113**(8), p. 082902, 2018.

[31] J. Lyu, I. Fina, R. Solanas, J. Fontcuberta, and F. Sánchez, "Growth window of ferroelectric epitaxial hf0. 5zr0. 5o2 thin films," *ACS Applied Electronic Materials* **1**(2), pp. 220–228, 2019.

[32] Y. Wei, S. Matzen, T. Maroutian, G. Agnus, M. Salverda, P. Nukala, Q. Chen, J. Ye, P. Lecoeur, and B. Noheda, "Magnetic tunnel junctions based on ferroelectric hf0.5zr0.5o2 tunnel barriers," *Physical Review Applied* **12**(3), p. 031001, 2019.

[33] M. C. Sulzbach, S. Estandía, X. Long, J. Lyu, N. Dix, J. Gàzquez, M. F. Chisholm, F. Sánchez, I. Fina, and J. Fontcuberta, "Unraveling ferroelectric polarization and ionic contributions to electroresistance in epitaxial hf0.5zr0.5o2 tunnel junctions," *Advanced Electronic Materials* , p. 1900852, 2019.

[34] D. Pantel, S. Goetze, D. Hesse, and M. Alexe, "Reversible electrical switching of spin polarization in multiferroic tunnel junctions," *Nature Materials* **11**(4), p. 289, 2012.

[35] Y. Yin, J. Burton, Y. M. Kim, A. Y. Borisevich, S. J. Pennycook, S. M. Yang, T. Noh, A. Gruverman, X. Li, E. Tsymbal, *et al.*, "Enhanced tunnelling electroresistance effect due to a ferroelectrically induced phase transition at a magnetic complex oxide interface," *Nature Materials* **12**(5), p. 397, 2013.

[36] J. M. De Teresa, A. Barthelemy, A. Fert, J. P. Contour, F. Montaigne, and P. Seneor, "Role of metal-oxide interface in determining the spin polarization of magnetic tunnel junctions," *Science* **286**(5439), pp. 507–509, 1999.

[37] P. LeClair, B. Hoex, H. Wieldraaijer, J. Kohlhepp, H. Swagten, and W. De Jonge, "Sign reversal of spin polarization in c o/r u/a l 2 o 3/co magnetic tunnel junctions," *Physical Review B* **64**(10), p. 100406, 2001.

[38] I. V. Marún, F. Postma, J. Lodder, and R. Jansen, "Tunneling magnetoresistance with positive and negative sign in la0.67sr0.33mno3/srtio3/co junctions," *Physical Review B* **76**(6), p. 064426, 2007.

[39] U. Bauer, M. Przybylski, J. Kirschner, and G. S. Beach, "Magnetoelectric charge trap memory," *Nano Letters* **12**(3), pp. 1437–1442, 2012.

[40] U. Bauer, S. Emori, and G. S. Beach, "Electric field control of domain wall propagation in pt/co/gdox films," *Applied Physics Letters* **100**(19), p. 192408, 2012.

[41] J. S. Moodera, J. Nassar, and G. Mathon, "Spin-tunneling in ferromagnetic junctions," *Annual Review of Materials Science* **29**(1), pp. 381–432, 1999.

[42] J. De Teresa, A. Barthélémy, A. Fert, J. Contour, R. Lyonnet, F. Montaigne, P. Seneor, and A. Vaures, "Inverse tunnel magnetoresistance in co/srtio3/la0.7sr0.3mno3: new ideas on spin-polarized tunneling," *Physical Review Letters* **82**(21), p. 4288, 1999.

[43] E. Y. Tsymbal, A. Sokolov, I. Sabirianov, and B. Doudin, "Resonant inversion of tunneling magnetoresistance," *Physical Review Letters* **90**(18), p. 186602, 2003.

[44] R. Cauro, A. Gilabert, J. Contour, R. Lyonnet, M.-G. Medici, J.-C. Grenet, C. Leighton, and I. K. Schuller, "Persistent and transient photoconductivity in oxygen-deficient la 2/3 sr 1/3 mno 3- δ thin films," *Physical Review B* **63**(17), p. 174423, 2001.

[45] C. Ge, K.-J. Jin, L. Gu, L.-C. Peng, Y.-S. Hu, H.-Z. Guo, H.-F. Shi, J.-K. Li, J.-O. Wang, X.-X. Guo, *et al.*, "Metal–insulator transition induced by oxygen vacancies from electrochemical reaction in ionic liquid-gated manganite films," *Advanced Materials Interfaces* **2**(17), p. 1500407, 2015.

[46] C. Schlueter, P. Orgiani, T.-L. Lee, A. Y. Petrov, A. Galdi, B. Davidson, J. Zegenhagen, and C. Aruta, "Evidence of electronic band redistribution in la 0.65 sr 0.35 mno 3- δ by hard x-ray photoelectron spectroscopy," *Physical Review B* **86**(15), p. 155102, 2012.

[47] L. Yao, S. Inkinen, and S. Van Dijken, "Direct observation of oxygen vacancy-driven structural and resistive phase transitions in la2/3sr1/3mno3," *Nature Communications* **8**, p. 14544, 2017.

[48] Q. H. Qin, L. Äkäslompolo, N. Tuomisto, L. Yao, S. Majumdar, J. Vijayakumar, A. Casiraghi, S. Inkinen, B. Chen, A. Zugarramurdi, *et al.*, "Resistive switching in all-oxide ferroelectric tunnel junctions with ionic interfaces," *Advanced Materials* **28**(32), pp. 6852–6859, 2016.

[49] R. Waser, R. Dittmann, G. Staikov, and K. Szot, "Redox-based resistive switching memories-nanoionic mechanisms, prospects, and challenges," *Advanced Materials* **21**(25-26), pp. 2632–2663, 2009.

[50] J. O'donnell, A. Andrus, S. Oh, E. Colla, and J. Eckstein, "Colossal magnetoresistance magnetic tunnel junctions grown by molecular-beam epitaxy," *Applied Physics Letters* **76**(14), pp. 1914–1916, 2000.

[51] A. Sawa, "Resistive switching in transition metal oxides," *Materials Today* **11**(6), pp. 28–36, 2008.

[52] R. Waser and M. Aono, "Nanoionics-based resistive switching memories," in *Nanoscience And Technology: A Collection of Reviews from Nature Journals*, pp. 158–165, World Scientific, 2010.

[53] S. Seo, M. Lee, D. Seo, E. Jeoung, D.-S. Suh, Y. Joung, I. Yoo, I. Hwang, S. Kim, I. Byun, *et al.*, "Reproducible resistance switching in polycrystalline nio films," *Applied Physics Letters* **85**(23), pp. 5655–5657, 2004.

[54] J. Simmons and R. Verderber, "New conduction and reversible memory phenomena in thin insulating films," *Proceedings of the Royal Society of London. Series A. Mathematical and Physical Sciences* **301**(1464), pp. 77–102, 1967.

[55] B. Choi, D. S. Jeong, S. Kim, C. Rohde, S. Choi, J. Oh, H. Kim, C. Hwang, K. Szot, R. Waser, *et al.*, "Resistive switching mechanism of tio2 thin films grown by atomic-layer deposition," *Journal of Applied Physics* **98**(3), p. 033715, 2005.

[56] A. Gruverman, D. Wu, H. Lu, Y. Wang, H. Jang, C. Folkman, M. Y. Zhuravlev, D. Felker, M. Rzchowski, C.-B. Eom, *et al.*, "Tunneling electroresistance effect in ferroelectric tunnel junctions at the nanoscale," *Nano Letters* **9**(10), pp. 3539–3543, 2009.

[57] M. Hoffmann, U. Schroeder, T. Schenk, T. Shimizu, H. Funakubo, O. Sakata, D. Pohl, M. Drescher, C. Adelmann, R. Materlik, *et al.*, "Stabilizing the ferroelectric phase in doped hafnium oxide," *Journal of Applied Physics* **118**(7), p. 072006, 2015.

[58] S. Starschich, S. Menzel, and U. Böttger, "Evidence for oxygen vacancies movement during wake-up in ferroelectric hafnium oxide," *Applied Physics Letters* **108**(3), p. 032903, 2016.

[59] S. Valencia, A. Crassous, L. Bocher, V. Garcia, X. Moya, R. Cherifi, C. Deranlot, K. Bouzehouane, S. Fusil, A. Zobelli, *et al.*, "Interface-induced room-temperature multiferroicity in batio3," *Nature Materials* **10**(10), p. 753, 2011.

[60] S. Zhang, "Spin-dependent surface screening in ferromagnets and magnetic tunnel junctions," *Physical Review Letters* **83**(3), p. 640, 1999.

[61] M. Y. Zhuravlev, S. Maekawa, and E. Y. Tsymbal, "Effect of spin-dependent screening on tunneling electroresistance and tunneling magnetoresistance in multiferroic tunnel junctions," *Physical Review B* **81**(10), p. 104419, 2010.

[62] M. Bowen, J.-L. Maurice, A. Barthélémy, P. Prod'homme, E. Jacquet, J.-P. Contour, D. Imhoff, and C. Colliex, "Bias-crafted magnetic tunnel junctions with bistable spin-dependent states," *Applied Physics Letters* **89**(10), p. 103517, 2006.

[63] K. Klyukin, L. Tao, E. Y. Tsymbal, and V. Alexandrov, "Defect-assisted tunneling electroresistance in ferroelectric tunnel junctions," *Physical Review Letters* **121**(5), p. 056601, 2018.